Estimates of Power Consumed by Mixing in the Ocean Interior

LOUIS ST. LAURENT

Department of Oceanography, The Florida State University, Tallahassee, Florida

HARPER SIMMONS

International Arctic Research Center, University of Alaska Fairbanks, Fairbanks, Alaska

(Manuscript received 6 September 2005, in final form 17 January 2006)

ABSTRACT

Much attention has focused on the power required for driving mixing processes in the ocean interior, the thermohaline circulation, and the related meridional overturning circulation (MOC). Recent estimates range from roughly 0.5 to 2 TW (1 TW = 1×10^{12} W), based on differing arguments for the closure of the MOC mass budget. While these values are both $O(1)$ TW, the thermodynamic implications of the estimates are significantly different. In addition, these numbers represent an integral constraint on the global circulation, and the apparent discrepancy merits careful examination. Through basic thermodynamic considerations on water mass mixing, a mechanical power consumption of 3 ± 1 TW is found to be consistent with a basic knowledge of the distribution and magnitude of oceanic turbulence diffusivities. This estimate is somewhat independent of any specific model for mass closure of the MOC. In addition, this estimate is based on a thermocline diffusivity of only 0.1 $cm^2\ s^{-1}$, with enhanced diffusivities acting only in the deep and bottom waters. Adding enhanced diffusivities in the upper ocean, or lowering the mixing efficiency below 20%, will increase the power estimate. Moreover, 3 TW is a reasonable estimate for the power availability to processes acting beneath the oceanic mixed layer.

1. Introduction

In what we will term the "traditional" view, the meridional overturning circulation (MOC) of the ocean is assumed to close through diabatic processes in the ocean interior. In this case, turbulent mixing in the ocean interior acts to transfer heat from the temperate waters of the upper ocean to the colder waters of the abyss. This heat transfer acts to modify the deep and bottom water masses of the abyss: North Atlantic Deep Water (NADW) and Antarctic Bottom Water (AABW). The buoyancy exchanged by mixing is thought to result in a net upwelling of dense fluid within the abyssal ocean (Fig. 1). In a global average sense, this conversion and upwelling of abyssal water balances the production of deep water at high latitudes. Thus, the ocean's density structure is allowed to remain in steady state. The basic elements of this balance between advection and diffusion were presented by Munk (1966) though the general concept can be found in earlier studies (Stommel 1957; Wyrtki 1961). Munk's article also showed that an upwelling rate of $w_* = 1 \times 10^{-7}$ m s^{-1} and a turbulent diffusivity of $k_\upsilon = 1 \times 10^{-4}$ $m^2\ s^{-1}$ were consistent with basin-scale average distributions of temperature and tracers for the waters *deeper than 1 km*. The latter consideration is often neglected in discussions of ocean mixing, leading many to suggest that there is "missing mixing" in the upper ocean where diffusivities are observed to be an order of magnitude less (Kerr 2000; Hughes and Griffiths 2006). We shall argue later that contemporary estimates of mixing rates for the various water masses do not necessarily lead to a missing mixing dilemma.

Munk and Wunsch (1998) reexamined the calculations of Munk (1966). Rather than inferring k_υ and w^* from observed tracer profiles, they examined the parameters that allow for the diabatic upwelling of 25×10^6 $m^3\ s^{-1}$ of deep water in the oceanic interior. As in Munk (1966), $k_\upsilon \approx 1 \times 10^{-4}$ $m^2\ s^{-1}$ was found to be a reasonable global average diffusivity for depths great than 1 km. Munk and Wunsch considered the mechani-

Corresponding author address: Dr. Louis St. Laurent, Department of Oceanography, The Florida State University, Rm. 407 OSB, Tallahassee, FL 32606-4320.
E-mail: lous@ocean.fsu.edu

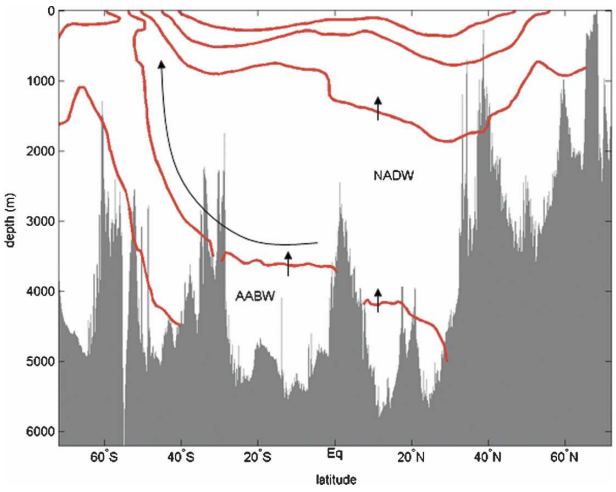

FIG. 1. Section of potential temperature along 30°W in the Atlantic Ocean. Isotherms for 0°, 2°, 4°, 10°, and 15°C are shown, as computed from the *World Ocean Atlas* of Levitus and Boyer (1994). The AABW and NADW masses are labeled. Internal mixing in the abyss is thought to add buoyancy to cause upwelling, as indicated by upward arrows. An additional upwelling pathway for NADW is adiabatic, involving advection southward toward the outcrop region of the Southern Ocean.

cal energy budget needed for the turbulent dissipation associated with this mixing requirement. They based their estimates on the concept of a mixing efficiency for turbulence, where the ratio between buoyancy flux and the dissipated energy is taken as 20% (Osborn 1980). Munk and Wunsch estimate that 2.1 TW (1 TW = 1×10^{12} W) of mechanical energy is dissipated to support an abyssal diffusivity of 1×10^{-4} m^2 s^{-1}. This abyssal power requirement appears to be in addition to the energy required for weaker thermocline mixing, which they estimated as 0.2 TW. This latter value appears to be an underestimate by a factor of 2–3, owing to the approximate method Munk and Wunsch used for integrating the oceanic buoyancy field.

In an apparently conflicting alternative view, the MOC can be closed with only minimal mixing in the ocean's interior. An adiabatic closure is conceptualized as largely occurring through upwelling in the Southern Ocean (Fig. 1). There, dense waters of North Atlantic origin (primarily of NADW) can rise to the surface under the direct influence of the wind-forced surface mixed layer. In this view, mixing in the ocean interior is required mainly for the densest waters of the global ocean. This Southern Ocean pathway was demonstrated in the idealized numerical simulations of Toggweiler and Samuels (1998), and in recent theoretically motivated studies (Marshall and Radko 2003). An estimate of the power required for mixing was presented by Webb and Suginohara (2001a,b), who suggest that less than 0.6 TW of mechanical energy is needed for mixing these densest waters. Their calculation appears to be based on the presumption that roughly 75% of the MOC mass closure of the NADW density class occurs in the region of the Southern Ocean subpolar front. Scaling accordingly, this leaves only 25% of the Munk and Wunsch (1998) 2.1-TW mechanical energy dissipation as actually needed for diabatic mixing processes in the oceanic interior. Gnanadesilean et al. (2005) extend the ideas of Webb and Suginohara, suggesting that eddy fluxes of buoyancy are the critical process in this scenario. Further work by Hughes and Griffiths (2006) has suggested that entrainment processes in high-latitude regions act directly during deep-water formation to reduce the amount of mechanical mixing needed in the ocean interior. Their conceptual model suggests that only 10% of the Munk and Wunsch (1998) estimate of mechanical power is needed for the MOC.

These estimates indicate a significant dilemma in our current understanding of the ocean's physics. The net power consumed by mixing in the ocean interior represents a global integral constraint on the thermodynamics of the ocean interior. In one sense, these estimates are not significantly different in magnitude, as both are $O(1)$ TW. However, the contrast in ocean physics separating these two scenarios is significant (diabatic versus adiabatic for much of the deep ocean), and our understanding of the ocean should be sufficient to resolve the difference. It is important to note that both estimates are motivated by closure requirements of the MOC mass budget through upwelling, with mixing levels and energy requirements following as secondary estimates. There are good reasons for pursuing the problem in this way, as the mass closure constraint is one of the most fundamental in any fluid mechanical system. However, given the discrepancy between contemporary views, it is also useful to examine an estimate deriving from purely thermodynamic considerations. This serves as the motivation for our study.

Here, we shall examine the power consumed by mixing processes in the ocean interior. Previous estimates started from an assumed rate of deep-water production and then inferred an ocean interior mixing rate needed for upwelling (full or partial) in the overturning circulation. We shall discuss a different approach, where diffusivities are taken based on prior estimates, and the power consumption is estimated though basic thermodynamic relations involving the mixing efficiency.

Estimates of turbulent mixing in the ocean interior

Munk's suggestion of an advection–diffusion balance in the ocean's deep interior motivated nearly 40 yr of ocean mixing studies. In particular, the suggestion that

diffusivities are $O(1 \times 10^{-4})$ m^2 s^{-1} served as an observational Holy Grail.[1] Starting with the seminal work of Osborn and Cox (1972), techniques have been developed to measure the dissipation rates of oceanic turbulence. The dissipation rates of thermal variance (χ) and kinetic energy (ε) are derived from small-scale fluctuations of temperature and velocity, leading to the term "microstructure" as a description of these measurements. These fluctuations need to be observed at scales approaching the Kolmogorov scale of turbulence (Kolmogorov 1941), typically $O(1)$ mm to $O(1)$ cm. In general, the kinetic energy dissipation rate (ε) is used to estimate the diffusivity through a model for buoyancy flux and mixing efficiency, as presented in section 2. Further details of contemporary microstructure methods are given by Davis (1994) and Lueck et al. (2002).

Following Osborn and Cox, many studies have employed measurements of microstructure to estimate diffusivities. Here, we will limit our discussion to only those studies that have examined turbulent mixing in the stratified interior of the deep ocean. Estimates of microstructure exclusive to observations of the mixed layer will not be considered. We will also not consider studies of mixing on the continental shelf or small regional seas, as these regions may lack a clear connection to the deep-ocean stratification and the MOC. This leaves approximately a dozen major studies of open-ocean mixing processes with observations at thermocline and abyssal depths. A summary of these data is given in Table 1. We admit that this may be an incomplete listing. We have also intentionally focused on data where $O(100)$ or more dissipation profiles were collected over periods from weeks to months, as these data allow for meaningful estimates of average diffusivities with depth.

In all cases in Table 1, dissipation rates were estimated from velocity microstructure (ε) measured at thermocline depths ($z > -1000$ m) and generally much deeper. Early microstructure measurements, including many studies not listed, were limited to this upper-ocean region. Deep profiling, particularly to depths greater than 2000 m, did not become common practice until the 1990s (Toole et al. 1994). It is also apparent that the open-ocean microstructure collection remains sparse. As discussed by Hibiya et al. (2002), the record favors low latitudes and summer periods. These limitations noted, the trend of mixing rates with depth appears to be robust, with $O(1 \times 10^{-5})$ m^2 s^{-1} diffusivities for the thermocline and $O(1\text{–}10) \times 10^{-4}$ m^2 s^{-1} for deep and abyssal water masses.

The North Atlantic Tracer Release Experiment (NATRE) program deserves special mention, as it was the first direct tracer-release experiment where average diffusivities were independently determined and compared with the microstructure-derived estimates (Ledwell et al. 1993). Despite nearly 20 yr of microstructure results prior to NATRE, it was this experiment that established confidence in the microstructure estimates. NATRE also showed that the thermocline diffusivity of $O(1 \times 10^{-5})$ m^2 s^{-1} based on early microstructure estimates (Gregg 1987) was sensible. Prior to this direct confirmation, microstructure estimates were often questioned for not agreeing with Munk's value (Davis 1994, 1996).

Microstructure-based methods have also yielded "finestructure" parameterizations, which typically relate shear and strain of the oceanic internal wave field to dissipation (Gregg 1989; Polzin et al. 1995). This has allowed for the estimation of turbulent diffusivities based on measurements from standard nonmicrostructure survey instrumentation, such as conductivity–temperature–depth systems (CTDs) and lowered Acoustic Doppler Current Profilers (LADCPs) now widely in use (Polzin et al. 2002). Mauritzen et al. (2002) applied a density finestructure parameterization to a hydrographic section along 11°N in the Atlantic, inferring diffusivities of $O(1\text{–}10) \times 10^{-4}$ m^2 s^{-1} in the deep and bottom water above the Mid-Atlantic Ridge. Polzin and Firing (1997) were the first to employ the shear-based parameterization to LADCP data. They examined the WOCE "I8" section across the Antarctic Circumpolar Current (ACC), and estimated $k_\upsilon \approx O(1\text{–}10) \times 10^{-4}$ m^2 s^{-1} for the full 5000 m of ocean depth for the region between 50° and 60°S. Naveira Garabato et al. (2004) employed a finestructure parameterization to CTD/LADCP sections in the Scotia Sea region of the Southern Ocean, suggesting diffusivities as large as $O(10 \times 10^{-4})$ m^2 s^{-1} in the deep- and bottom-water classes there. Kunze et al. (2006) have further employed a shear/strain parameterization to nearly 3500 CTD/LADCP profiles around the globe. They find generally mixing rates of $O(1 \times 10^{-5})$ m^2 s^{-1} in many regions, though larger mixing rates are typical in the high-latitude regions.

Direct measurements and finestructure parameterizations have a significant limitation. Both are generally unable to be used to define basin-scale averages, as measurements are generally too sparse for such large

[1] This value of diffusivity has the useful conversion to cgs units of 1 cm^2 s^{-1}. This unit of diffusivity was respectfully named "the Munk unit" (1 Munk = 1 cm^2 s^{-1} = 1×10^{-4} m^2 s^{-1}) at the IAPSO/SCOR Symposium on Ocean Mixing held in Victoria, British Columbia, Canada during October 2004. For easy reference, we will express all diffusivity estimates as multiples of 1×10^{-4} m^2 s^{-1}.

TABLE 1. Listing of open-ocean microstructure studies. Location coordinates are only approximate and generally indicate a reference point to a spatial survey. Diffusivities are given as order of magnitudes.

Program/expt	Location	Dates	Diffusivities $O(\times 10^{-4})$ m^2 s^{-1}	Notes	References
Wespac	North Pacific 35°N, 152°E	May 1982	0.1 (in the thermocline) 1 ($z \approx 2000$ m)	First deep microstructure observations	Moum and Osborn (1986)
C-SALT/ SFTRE	Equatorial Atlantic 12°N, 56°W	Nov 1985 Jan 2001	0.1 (above/below the staircase) 1 (in the staircase)	Double-diffusive staircase region	Schmitt et al. (2005)
PATCHEX	North Pacific 34°N, 127°W	Oct 1986	0.1 (in the thermocline)	Study focused on thermocline processes	Gregg (1989)
Tropic Heat 1/Tropic Heat 2	Equatorial Pacific 0°, 140°W	Apr 1984 Feb 1987	0.1 (in the thermocline) 1 (in the undercurrent)	Studies focused on equatorial processes	Peters et al. (1989, 1994)
NATRE (Canary Basin)	North Atlantic 25°N, 30°W	Mar 1992	0.1 (thermocline) 1 (in NADW)	First open-ocean tracer release	Toole et al. (1994)
Cobb Seamount	North Pacific 46°N, 131°W	Jun 1994	0.1 (away from the seamount) 1 (above the seamount)	Study focused on mixing near seamount	Lueck and Mudge (1997)
Romanche Fracture Zone	Equatorial Atlantic 0°, 12°W	Nov 1994	0.1 (in thermocline) >10 (in AABW)	Study focused on fracture zone	Ferron et al. (1998)
Fieberling Guyot	North Pacific 32°N, 128°W	Apr 1991	0.1 (away from seamount) 1 (near seamount)	Study focused on mixing near seamount	Kunze and Toole (1997)
BBTRE (Brazil Basin)	South Atlantic 20°S, 15°W	Jan 1996 Mar 1997	0.1 (in the thermocline) 1 (in NADW) >10 (in AABW)	Basin-scale survey and tracer release	St. Laurent et al. (2001)
HOME	North Pacific 22°N, 159°W	Dec 2000 Oct 2002	0.1 (away from the ridge) 1 (near the ridge)	Study focused on mixing along Hawaiian Ridge	Klymak et al. (2006)

TABLE 2. Midlatitude estimates of diffusivity and power. Two cases of diffusivities described in previous studies are considered as cases A and B.

Water class	Diffusivity (k_v) ($\times 10^{-4}$ m^2 s^{-1}) power (P) (TW)	
	Case A: GW00	Case B: LS
Ventilated ($\gamma^n < 27.96$)	$k_v = 0.1$, $P = 0.55$	$k_v = 0.1$, $P = 0.55$
Deep water ($27.96 < \gamma^n < 28.1$)	$k_v = 3$, $P = 0.61$	$k_v = 1$, $P = 0.2$
Bottom water ($\gamma^n > 28.1$)	$k_v = 10$, $P = 0.49$	$k_v = 3$, $P = 0.15$
Total power	1.65	0.9

spatial areas. In particular, measurements in a basin's interior will underestimate the mean mixing rate for a water mass that experiences transformation in deep passages. Numerous studies have shown that diffusivities of $O(10–100) \times 10^{-4}$ m^2 s^{-1} occur in canyons and fracture zones (Ferron et al. 1998; St. Laurent et al. 2001; Bryden and Nurser 2003; Thurnherr et al. 2005).

Indirect estimates based on hydrographic inverse methods are the only method for inferring mixing rates for basin-scale regions. We characterize these into two somewhat subjective classes: algebraic inversions and statistical inversions. The former class involves calculations using the advective equations for mass and heat in simple control volumes. The equations are then solved algebraically for one or more mixing parameters. Often, control volumes are chosen for an abyssal water mass that is contained in a semienclosed basin. Hogg et al. (1982) used such techniques with hydrographic and current meter data from the abyssal Brazil Basin. There, much of the circulation is controlled by several deep gaps and fracture zones (Vema, Romanche, etc). The use of current meter records from these passages, and hydrographic measurements of the basin interior, allowed Hogg et al. (1982) to derive mixing rates for the deepest water masses of the Brazil Basin. Morris et al. (2001) revisited these earlier calculations using the World Ocean Circulation Experiment (WOCE) era hydrography, allowing for some comparison to the Brazil Basin Tracer Release Experiment (BBTRE) microstructure (St. Laurent et al. 2001). Heywood et al. (2002) also used a control volume method to calculate diffusivity for the enclosed basin of the Scotia Sea. They estimate a basin average diffusivity of 40×10^{-4} m^2 s^{-1} for the AABW in this region.

Statistical inversions deal with the solution of many advective equations for mass, heat, and other tracers, in complex control volumes that may involve middepth regions and the upper-ocean boundary layer. These problems are generally rank deficient to some degree, even in "overdetermined" cases where the number of equations exceeds the number of unknowns (Wunsch 1996). Early inversions focused on lateral advection only, as a means of solving the integration constant of the thermal wind equations (Wunsch 1978; Stommel and Schott 1977). More recent inversions have resolved vertical velocities, and also mixing parameters for lateral and vertical diffusion. In particular, WOCE era hydrography and tracer observations have proven valuable in resolving diapycnal diffusivities. Ganachaud and Wunsch (2000, hereafter GW00), following earlier work by MacDonald and Wunsch (1996), invert an impressive array of midlatitude tracer fields. Their estimates resolved diapycnal diffusivities in deep- and bottom-water layers, defined by neutral density, for all of the major midlatitude basins (Table 2). GW00 focus their analysis on the midlatitudes, between 30°S and 47°N, to avoid the complications of air–sea flux influence on the deep- and bottom-water classes. Lumpkin and Speer (2003) pursue a similar inversion for the Atlantic only, but extend their analysis to northern high latitudes with the inclusion of air–sea flux terms. Lumpkin and Speer (2006, manuscript submitted to *J. Phys. Oceanogr.*, hereafter LS) have additionally done a global inversion with explicit air–sea forcing, allowing for estimates of diffusivity over a full range of latitudes. The LS estimates are subject to considerable uncertainty, propagated by the error estimates for the surface flux terms. Olbers and Wenzel (1989) specifically consider diffusivity estimates in the Southern Ocean. Their estimates are based on inversion of climatology, and they find $k_v \approx O(10 \times 10^{-4})$ m^2 s^{-1} in the lower 1 km of the ACC region.

While a full review of hydrographic inverse results is beyond the scope of the current study, a basic summary of the diapycnal diffusivities can be easily done. A thermocline diffusivity of 1×10^{-5} m^2 s^{-1} is now well established, with reference to the numerous studies cited in Table 1. Contemporary inverse estimates of thermocline diffusivities also support this value (GW00; LS). For deep-water diffusivities, direct estimates are scarce, and even scarcer for bottom water. In addition to the small number of microstructure-based estimates cited in Table 1, inverse studies are the primary base of knowledge for vertical diffusivities of the dense water classes. These, along with the direct measurements, indicate a marked increase in mixing rates below the ven-

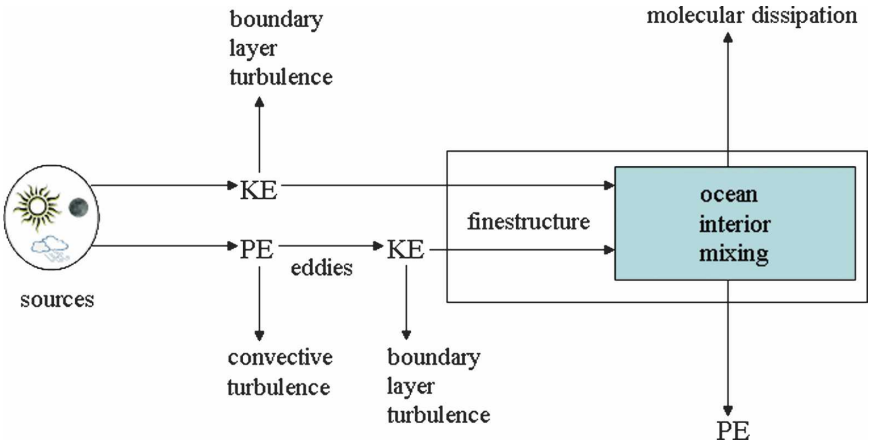

FIG. 2. Diagram showing the cascade of energy from sources to sinks. Both kinetic energy (KE) and potential energy (PE) pathways are possible. Some energy may be dissipated in boundary layers or in convective turbulence. Some energy is also cascaded to finestructure such as the internal wave field. We assume that all finestructure energy is either directly dissipated or converted to buoyancy flux (converted to PE) by turbulence.

tilated waters of the thermocline. The GW00 basin-scale estimates are $k_\upsilon \approx (3 \pm 1) \times 10^{-4}$ m^2 s^{-1} for deep water, and $k_\upsilon \approx (10 \pm 3) \times 10^{-4}$ m^2 s^{-1} for bottom water. In their research, LS find $k_\upsilon \approx$ (1–3) $\times 10^{-4}$ for these water masses, with uncertainties comparable to the mean estimates.

Finally, modeling studies have also been used to examine the distribution of mixing in numerical ocean general circulation models (OGCMs). Often studies involve the ad hoc specification of diffusivities. Models ranging in geometric sophistication from a closed-box sector (Bryan 1987) to a full OGCM (Hasumi and Suginohara 1999) have been used to study the effects of vertical diffusion. Other studies have a priori assumed adiabatic conditions with no explicit turbulent diffusion, such as in the idealized sector-based Southern Ocean geometry simulations of Toggweiler and Samuels (1998). In practice, nearly all OGCM climate simulations are subject to nontrivial levels of diffusion due to numerical effects (Griffies et al. 2000). Models employing physically based parameterizations for the specification of diffusivities including turbulence closure schemes (Canuto et al. 2002) and energy budget closure (Simmons et al. 2004) have been proposed. The study by Simmons et al. (2004) is the most relevant to the problem examined in this paper, as their calculations considered a mixing rate parameterization based in the mechanical energy available from deep-ocean internal tides. OGCM studies are clearly important, as they represent the only mechanism for assessing the effects of mixing on the large-scale properties of the ocean. However, OGCMs are not a proven tool for predicting the distribution of mixing. In the present study, we focus only on data-based diffusivity results.

We conclude this brief review of prior mixing rate estimates by commenting on the missing mixing described by some previous studies, where a discrepancy is cited between budget-derived average mixing rates and directly measured diffusivities. Often the classical Munk (1966) estimate of $k_\upsilon \approx 1 \times 10^{-4}$ m^2 s^{-1} is contrasted to direct measurements in the thermocline (e.g., Ledwell et al. 1993). In such comparisons, the *abyssal* context of the Munk estimate is generally overlooked. As can be seen through inspection of Table 1, direct measurements of deep diffusivities generally exceed $O(1 \times 10^{-4})$ m^2 s^{-1} in magnitude, consistent with the classic Munk reference. At thermocline depths, early ideas about a diffusive thermocline (e.g., Robinson and Stommel 1959) have been abandoned for weakly diffusive models (e.g., Samelson and Vallis 1997). There is now general agreement that weak mixing levels observed in the thermocline are not in error. Instead, there is now recognition that strong variations in turbulence levels occur between the thermocline and abyssal water masses.

2. Governing thermodynamics

We will present the most basic model of a steady-state mechanical energy balance for sustaining turbulent mixing in the ocean interior. This model does not consider the full cascade of energy from the scale of the forcing to that of dissipation. Instead, we consider only the energy exchange between finestructure and dissipation (Fig. 2). We do not discern between the various

sources that cascade energy into finestructure, and both potential and kinetic energy sources are possible. Furthermore, our model is intended to quantify dissipation only in the stratified oceanic interior. Dissipation occurring in the surface mixed layer and in frictional boundary layers will not be considered here.

Consider a control volume for a basin-scale region. Turbulent mixing occurring in the basin is the result of many individual events, intermittent in time and space. Here, we consider only the ensemble statistics through integrating over many events contained in a basin-scale control volume (dV). The steady-state balance for turbulent kinetic energy over this control-volume ensemble can be written as

$$\int P\,dV = \int \rho\varepsilon\,dV + \int \rho k_v N^2\,dV, \tag{1}$$

where P is the mechanical power supplied to finestructure scales. For steady-state conditions to exist, power is either directly dissipated by the molecular viscosity of seawater (ε), or converted to potential energy through turbulent diffusion. We note that the total power input can be broken into multiple terms including power terms associated with mesoscale eddies (b_e) and convection (b_c),

$$\int (p + b_e + b_c)\,dV = \int \rho\varepsilon\,dV + \int k_v N^2\,dV, \tag{2}$$

where p represents any direct flux of mechanical energy to finestructure, such as internal waves. Given knowledge of the turbulent diffusivity and the stratification (N^2), a relationship between k_v and ε is required to determine the integrated power input. The concept of "mixing efficiency" is often used for this purpose (Osborn 1980). The mixing efficiency is formally defined as the ratio of buoyancy flux (J_b) to power and is identified as the *flux* Richardson number ($R_f = J_b/P$). An alternate efficiency parameter gives the ratio of buoyancy flux to dissipation, $\Gamma = J_b/\varepsilon$. This efficiency parameter is directly related to the flux Richardson number, $\Gamma = R_f/(1 - R_f)$. We will use the integral definition for an ensemble of many events,

$$\Gamma = \frac{\int \rho k_v N^2\,dV}{\int \rho\varepsilon\,dV}. \tag{3}$$

This parameter has been quantified in many oceanographic settings, including the mixed layer (Oakey 1985), the thermocline (Moum 1996), and in doubly stable and double-diffusive regions (St. Laurent and Schmitt 1999). Laboratory work (Rohr and Van Atta 1987) and theoretical calculations (Thompson 1980) have also quantified the mixing efficiency of turbulence. In general, a value of $\Gamma = 0.2$ is accepted as typical for mixing by shear instability (Peltier and Caulfield 2003). However, arguments for a lower mixing efficiency have also been made (Huq and Britter 1995; Stigebrandt and Aure 1989; Arneborg 2002). These studies suggest $\Gamma = 0.05$–0.1. For now, we proceed with the idea that an efficiency parameter of roughly 20% is useful for examining the energy needed for turbulent mixing. The consequences of adopting lower values of mixing efficiency will be discussed later (section 4c).

Given (3), the dissipation is readily expressed in terms of the diffusivity. From (1), the total power is

$$\int P\,dV = \left(\frac{1}{\Gamma} + 1\right)\int \rho k_v N^2\,dV\,. \tag{4}$$

The dependence of (4) on Γ^{-1} indicates that an increasing power input is needed to achieve a given buoyancy flux for a decreasing mixing efficiency. Our estimates will depend on applying a mixing efficiency value appropriate for turbulence. We must neglect purely convective mixing where $P = 0$ in (1), leaving only the balance between buoyancy flux and dissipation. This means that convection in the upper boundary layer, and also double diffusive convection at depth, will be neglected in our calculations.

3. Methods

Here, we present an alternative to previous studies for the estimate of the power consumed by mixing in the oceanic interior. Unlike the previous estimates, our calculation is independent of an a priori upwelling rate of deep water. Instead, we start from estimates of the mixing rate, and consider only the mechanical energy needed to support turbulent mixing according to (4). From the onset, we will neglect the dissipation of energy that occurs in the oceanic boundary layers. This includes neglect of the frictional boundary layers at the oceanic margins, such as the bottom boundary layer in most regions, and all continental shelf regions with depths shallower than 100 m. These regions tend to be weakly stratified, and are not clearly connected to the density structure of the deep ocean. In addition, we neglect the power dissipated in the oceanic mixed layer, where enormous amounts of energy are removed through a litany of processes, including convective mixing (Wang and Huang 2004a,b). Extreme high-latitude regions are also excluded in our analysis, as these regions are the dominant sites of convective deep-water production. Specifically, we excluded regions north of 60°N and south of 65°S from our power estimates.

Our calculations begin by identifying the control vol-

umes over which the integration in (4) is performed. We adopt control volumes distinguished by neutral density, and we use the same layers considered by GW00 in their inverse calculations. Specifically, deep and bottom waters are identified as $27.96 < \gamma^n < 28.1$ and $\gamma^n > 28.1$ kg m^{-3} respectively. We further identify $\gamma^n < 27.96$ kg m^{-3} with the ventilated waters of the upper ocean. Density structure on the global scale of the oceanic basins was assessed using the *World Ocean Atlas* climatological data (Levitus and Boyer 1994; Levitus et al. 1994). Neutral density was calculated using the Jackett and McDougall (1997) algorithm, and the control volumes described above were mapped as spatial functions of the form $\gamma^n(x, y, z)$. Representative sections for the Atlantic, Pacific, and Indian Ocean sectors are shown in Fig. 3. The Atlantic section shown in Fig. 3a can be compared to the section shown in Fig. 1, with the 27.96 and 28.1 kg m^{-3} surfaces roughly corresponding to the 2° and 4°C isotherms. Notable differences arise when comparing basin-scale potential temperature to neutral density due to the role of salinity in density, and also due to significant differences in the way compressibility is treated in these quantities (Jackett and McDougall 1997).

Power estimates within each control volume follow from the assignment of an average diffusivity value, treated as a constant within the given density class. This leaves only the stratification term in the integral,

$$\int P\, dV = \rho k_v \left(\frac{1}{\Gamma} + 1\right) \int N^2\, dV\,. \tag{5}$$

It is important to recognize that (5) cannot be rewritten as simply involving the integral the surface and bottom density fields; that is, $\int N^2 dV \neq \int (\rho_{\text{top}} - \rho_{\text{bot}})\, dx\, dy$. This is due to the fact that the buoyancy gradient is not defined through any single density variable, but is instead calculated for a given buoyancy profile using a locally defined potential density that varies with depth. This technique is commonly known as "adiabatic leveling" (Fofonoff 1985; Millard et al. 1990). Our calculations thus involve calculation of $N^2(x, y, z)$ from the climatology, and then proceed with the integral over depth, which can be represented as a water column sum of locally defined potential buoyancy anomaly, $\int N^2\, dz = \Sigma_i \Delta b_i$. This summation actually mitigates the problems with local static instabilities in the climatologically based N^2 estimates (T. McDougall 2004, personal communication).

In our calculations, the mixing efficiency parameter is taken as $\Gamma = 0.2$ everywhere. We shall explore the implications of this choice below, as well as uncertainty in the diffusivity estimates. In addition to distinguishing

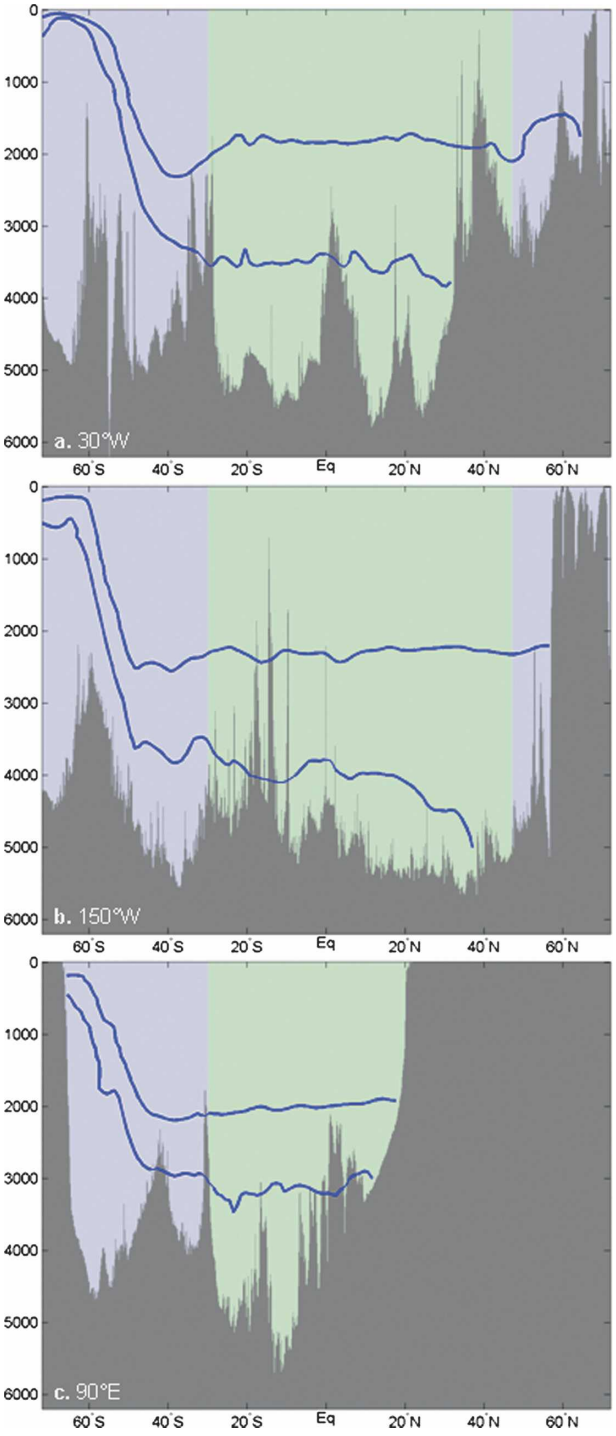

FIG. 3. Sections showing the ventilated-, deep-, and bottom-water density layers (as defined by $\gamma^n = 27.96$ and 28.1 kg m^{-3} neutral density surfaces) along (a) 30°W in the Atlantic, (b) 150°W in the Pacific, and (c) 90°E in the Indian Ocean. Shading indicates the mid- and high-latitude zones used by GW00. Bathymetry from Smith and Sandwell (1997) is shown (a)–(c). The influence of the Southern Ocean is indicated by the outcrop region of the neutral density contours.

control volumes by density layers, we also partition the control volumes into the midlatitude region between 30°S and 47°N, and the residual high-latitude regions to the north and south. This allows us to keep the power estimates in the high-latitude ocean separate, as the diffusivity estimates in GW00 were not formally derived for these regions.

In some past studies, precise values are reported for specific regions (e.g., Morris et al. 2001). In other cases, diffusivity estimates are given approximately, and likely useful only as order-of-magnitude estimates (e.g., Kunze et al. 2006). In all but global-scale statistical inversions, estimates from one or more studies must be extrapolated for application to the full ocean. Unfortunately, a collection of estimates from several studies generally show a range of diffusivities for a given water mass. Our power calculations are done using approximate estimates of diffusivity. In cases where diffusivity estimates range between integer powers of 10, we have used multiples of 3 in our calculations, such as $k_\upsilon \approx 3 \times 10^{-4}$ m^2 s^{-1} for the range $O(1\text{–}10) \times 10^{-4}$ m^2 s^{-1}. Power requirements calculated from (5) are reported in Terawatts for the full integration in each layer over all basins.

Uncertainty analysis for our estimates can be broken into two classes; parameter uncertainty and model uncertainty. Parameter uncertainty can be assessed through error propagation techniques (e.g., Bevington and Robinson 1992). For example, the standard error for the power estimate in (5) is given by

$$\delta P = P\left\{\left(\frac{\delta k_\upsilon}{k_\upsilon}\right)^2 + \left[\frac{\delta\Gamma}{\Gamma(1+\Gamma)}\right]^2 + \left(\frac{\delta\overline{N^2}}{\overline{N^2}}\right)^2\right\}^{1/2}, \tag{6}$$

where δk_υ, $\delta\Gamma$, and $\delta\overline{N^2}$, are the standard error estimates for the diffusivity, mixing efficiency parameter, and control-volume-averaged buoyancy gradient, respectively. Estimates of uncertainty for diffusivity are typically 25%–50% of the diffusivity magnitude, though specific details vary by study. The mixing efficiency parameter is generally treated as a theoretically specified value, though St. Laurent and Schmitt (1999) found $\delta\Gamma = 0.04$ in their microstructure-based analysis. The buoyancy gradient uncertainty is computed from the statistics of spatial variations in the density field. For the large-scale average buoyancy gradients used in the control-volume power calculation, $\delta\overline{N^2}/\overline{N^2} \approx 0.2$. Taking $\delta k_\upsilon/k_\upsilon \approx 0.25$ as typical of large-scale inversion estimates (e.g., GW00), with $\delta\Gamma/\Gamma \approx 0.25$ and $\delta\overline{N^2}/\overline{N^2} \approx 0.2$, a typical control-volume uncertainty estimate from (6) is $\delta P/P \approx 0.4$.

Given this general assessment of parameter uncertainty, the model uncertainties associated with diffusivity and mixing efficiency are more significant. Model uncertainty is used here to describe the systematic differences in diffusivity of mixing efficiency values found in different studies. For example, diffusivity estimates of various types (statistical or algebraic inverse models, finestructure parameterizations, or microstructure estimates) may reflect model uncertainty due to the subtleties of each form of estimation. In addition, the different studies suggesting $\Gamma \cong 0.5 - 0.1$ versus $\Gamma \cong 0.2$ cited above are also a form of model uncertainty. For simplicity of presentation, we proceed by documenting only the model error for control-volume power estimates when two cases of diffusivity estimation are considered for the midlatitudes (section 4a) and the high latitudes (section 4b). Model uncertainty for the mixing efficiency is considered in section 4c.

4. Results

a. Midlatitude estimates

Our midlatitude estimates are presented in Table 2. The sum of the power estimates for the entire midlatitude region is also reported. We have considered two sets of estimates; a primary estimate (Table 2, case A) motivated by GW00, and a secondary estimate (Table 2, case B) based on the study of LS. In applying the estimates of GW00, we use $k_\upsilon = 3 \times 10^{-4}$ m^2 s^{-1} for the deep-water class and $k_\upsilon = 10 \times 10^{-4}$ m^2 s^{-1} for the bottom-water class, noting that these values are slightly less than their actual estimates. A diffusivity of $k_\upsilon \approx 1 \times 10^{-5}$ m^2 s^{-1} was assigned for the ventilated water class ($\gamma^n < 27.96$ kg m^{-3}). There is roughly an even partition of power between the layers: 0.55, 0.61, and 0.49 TW for the ventilated, deep, and bottom waters, respectively. The total for this midlatitude region alone is 1.65 TW, already well above the 0.6-TW estimate of Webb and Suginohara (2001a,b).

Other studies have focused on deep and bottom water of the Atlantic basins, finding diffusivities between $(1\text{–}3) \times 10^{-4}$ m^2 s^{-1}. The study of Morris et al. (2001) examined diffusivities in the Brazil Basin using both an algebraic inversion and inferences made from microstructure. Lumpkin and Speer (2003) used a statistical inversion to estimate mixing rates through a larger region of the North and equatorial Atlantic basins. In their research LS find similar diffusivities in their global calculations. Based on these studies, we derive an alternative power estimate by assigning $k_\upsilon = 1 \times 10^{-4}$ m^2 s^{-1} and $k_\upsilon = 3 \times 10^{-4}$ m^2 s^{-1} for deep and bottom waters, respectively (Table 2, case B). This lowers the

TABLE 3. Southern Ocean estimates of diffusivity and power. Two cases of diffusivities described in previous studies are considered as cases A and B.

	Diffusivity (k_υ) ($\times 10^{-4}$ m^2 s^{-1}) power (P) (TW)	
Water class	Case A: Enhanced mixing studies: Olbers and Wenzel (1989), Polzin and Firing (1997), Heywood et al. (2002), Naveira Garabato et al. (2004)	Case B: Kunze et al. 2006; LS
Ventilated ($\gamma^n < 27.96$)	$k_\upsilon = 0.3$, $P = 0.24$	$K_\upsilon = 0.3$, $P = 0.24$
Deep water ($27.96 < \gamma^n < 28.1$)	$k_\upsilon = 3$, $P = 0.32$	$k_\upsilon = 1$, $P = 0.1$
Bottom water ($\gamma^n > 28.1$)	$k_\upsilon = 10$, $P = 0.79$	$k_\upsilon = 3$, $P = 0.3$
Total power	1.35	0.64

power estimates in the abyss, to 0.2 and 0.15 TW, thus lowering the midlatitude total to 0.9 TW.

b. High-latitude estimates

We have also considered various estimates of the power (5) for both the northern and southern high-latitude oceans. Our initial estimates for the northern oceans suggested that very little power is needed to support a plausible diffusivity distribution. Using the diffusivities of GW00, only 0.05 TW is needed for the region between 47° and 60°N. We note that this region represents only a small fraction of the global ocean area (less than 7%), and therefore contributes little relative to the global integral.

The Southern Ocean between 30° and 65°S occupies 20% of the global ocean area, and the power estimates there are significant. Diffusivity estimates for this region come from several sources, including both fine-structure–based parameterizations and algebraic and statistical inverse methods. We break the previous diffusivity estimates into two categories, those that indicate a general increase of k_υ with depth, and those that indicate a roughly depth-constant $k_\upsilon \approx O(1 \times 10^{-4})$ m^2 s^{-1}. In the former category, studies by Olbers and Wenzel (1989), Polzin and Firing (1997), Heywood et al. (2002), and Naveira Garabato et al. (2004), suggest order of magnitude increases of k_υ for the ventilated-, deep-, and bottom-water classes. Estimates for the ventilated waters are between $O(1\text{–}10) \times 10^{-5}$ m^2 s^{-1}, while estimates are between $O(1\text{–}10) \times 10^{-4}$ m^2 s^{-1} for the abyss. This distribution of diffusivity is similar to the GW00 estimates for midlatitudes, with the exception of the slightly larger Southern Ocean diffusivity for the upper ocean. We take $k_\upsilon = 0.3 \times 10^{-4}$, 3×10^{-4}, and 10×10^{-4} m^2 s^{-1} for the ventilated-, deep-, and bottom-water classes in our primary estimates of power (Table 2, case A). The associated estimates are 0.24, 0.32, and 0.79 TW, and thus contribute 1.35 TW to the global power integral.

Diffusivity estimates by Kunze et al. (2006) and LS suggest that mixing rates may be $O(1 \times 10^{-4})$ m^2 s^{-1} throughout the full depth in the circumpolar region. As an alternative to the estimate above, we calculate the power associated with $k_\upsilon = (0.3, 1, 3) \times 10^{-4}$ m^2 s^{-1} for the designated water classes in the Southern Ocean (Table 2, case B). Calculations for the various layers give 0.24, 0.1, and 0.3 TW for a total of 0.64 TW.

c. Model uncertainty for mixing efficiency

In formulating the model in Eqs. (1)–(4) we have relied on an assumed mixing efficiency, and have utilized $\Gamma = 0.2$. While direct measurements of turbulence often support this value, indirect estimates (Stigebrandt and Aure 1989) and theoretical estimates (Arneborg 2002) have suggested $\Gamma = 0.05$–0.1 is more appropriate. The minimal value was derived for the bottom waters of a weakly stratified fjord. St. Laurent et al. (2001) also found indirect evidence of $\Gamma = 0.05$ in deep abyssal canyons of the Brazil Basin. They suggest that such small mixing efficiencies may be characteristic of very weakly stratified turbulence. In contrast, Arneborg (2002) studied the case of fully stratified turbulence. His theoretically based estimates suggest that $\Gamma = 0.1$ is more appropriate for when the time average of an ensemble of turbulent mixing events is considered. Arneborg argues that the direct evidence supporting $\Gamma = 0.2$ is appropriate only for instantaneous observations of high turbulence. Reducing the efficiency parameter will increase the power estimates by roughly a factor of Γ^{-1}. Applying $\Gamma = 0.1$ to the bottom-water power estimates using the GW00 diffusivities (the case A analyses in Tables 2 and 3), we find 2.6 TW for $\gamma^n > 28.1$ (midlatitude and Southern Ocean) and 4.3 TW as a global total. A similar modification of the alternative estimates for bottom water (the case B estimates in Tables 2 and 3) gives 2 TW as a global estimate.

We note that additional permutations of varied diffusivity estimates and efficiency parameters are possible. However, the modest assessment of uncertainty offered above seems to capture the most obvious range

of parameters. We regard the case-A and case-B analyses of global power estimates as two possible degrees of freedom, and the adjustment of mixing efficiency for bottom water as a third degree of freedom. Taking the range of estimates for the 3 degrees of freedom as (4.4, 3.0, 2.0, 1.54) TW, we find a mean estimate of $P = 2.7 \pm 0.7$ TW.

5. Discussion

We have reviewed current knowledge of the diffusivity of turbulence diffusivities throughout the oceans. Estimates of this parameter come from several sources, including direct measurements, parameterizations of oceanic finestructure, and indirect estimates based on algebraic and statistical inversions of hydrography. While each of these methods require assumptions with potential limitations, results are generally consistent among water mass–based comparisons. Diffusivities in the ventilated waters of the thermocline are generally $k_\upsilon \approx 1 \times 10^{-5}$ m^2 s^{-1}, and mixing rates in the deep and bottom waters of the abyssal ocean are generally $O(1\text{–}10) \times 10^{-4}$ m^2 s^{-1}.

Given the summarized knowledge of turbulent diffusivities, we propose a new approach to quantifying the power needed for driving mixing in the ocean interior. We base our estimates on our existing estimates of turbulent diffusivities, using values from a variety of studies and methods. Our estimate of total power also relies on a model that relates turbulent buoyancy flux and dissipation by an efficiency parameter Γ. With this assumption, the power estimates follow directly as a thermodynamic result. This is in contrast to previous studies, which consider the mass closure requirements of the MOC and infer mixing rates, and hence power estimates, from the diabatic upwelling implied for the interior. As we have outlined in the introduction, two different scenarios arise from such reasoning. Our estimate clearly favors the more diabatic estimate of Munk and Wunsch (1998).

It is important to note that our method does not explicitly assume anything about the nature of the MOC or upwelling, we simply estimate the power supply needed to account for the distribution of turbulent diffusivity. We make no particular claim about the dynamics of the thermohaline circulation, and the MOC mass closure of the type described by Toggweiler and Samuels (1998) and Webb and Suginohara (2001a,b) is still possible. The diffusivity distributions considered in this study do not give any information about upwelling in the abyss. An increase in diffusivity with depth generally indicates downwelling through the loss of buoyancy. This is specified by the thermodynamic relation for the advection and buoyancy flux,

$$\begin{aligned} w^* N^2 &\equiv \frac{\partial}{\partial z}\left(k_\upsilon N^2\right) \\ &\equiv k_\upsilon \frac{\partial N^2}{\partial z} + N^2 \frac{\partial k_\upsilon}{\partial z}. \end{aligned} \tag{7}$$

As discussed by Simmons et al. (2004), if diffusivity increases with depth, then upwelling is possible 1) near the seafloor, and 2) $k_\upsilon \partial N^2/\partial z > |N^2 \partial k_\upsilon/\partial z|$. The former is understood as the consequence of mixing buoyancy above the insulating seafloor, while the latter can occur at any depth provided that the term containing the buoyancy gradient is stronger than that containing diffusivity change with depth. Simmons et al. (2004) calculate the distribution of w^* in their OGCM simulation. Their diffusivity specification is similar to that described as case B in Table 2, and maps showing their estimates of w^* for the $\gamma^n = 27.96$ and 28.1 kg m^{-3} surfaces are shown in Fig. 4. The distribution of diapycnal advection is clearly complex and nonuniform. Downwelling and upwelling occur over comparable areas throughout the mid- and low latitudes. Thus, it seems likely that simple conceptual ideas about a one-dimensional advective–diffusive balance in the abyssal interior are not constructive for describing the MOC. Instead, the MOC mass closure must occur through a spatially complex combination of upwelling and downwelling.

Our method is also insensitive to the particular details of any cascade process that provides power to the finescale. Instead, we assume that realistic energy sources and cascade pathways must exist to account for the $P = 3 \pm 1$ TW of power we have estimated. Sources of energy that can provide mechanical power to the oceanic interior include the winds (Wunsch 1998; Alford 2001, 2003) and tides (Egbert and Ray 2000; Jayne and St. Laurent 2001). Cascade pathways for these sources generally involve internal waves. The pathway by which subinertial winds transfer energy into the interior remain obscure, but may involve the transfer of potential energy released from the mesoscale eddy field, as schematically represented in Fig. 2. Kinetic energy input by marine biosphere has also been implicated as a mechanism by which chemical potential energy arising from primary production in the euphotic zone is converted to mechanical energy (Munk 1966; Dewar et al. 2006).

Estimates for these power inputs have various levels of uncertainty. Total wind energy input at the sea surface has been estimated in the range of 36 TW (Lueck and Reid 1984) to 60 TW (Wang and Huang 2004a,b). Nearly all of this energy is used or dissipated in mixed layer processes, and only $O(1)$ TW is estimated as flux into the interior (Alford 2001, 2003). The total tidal

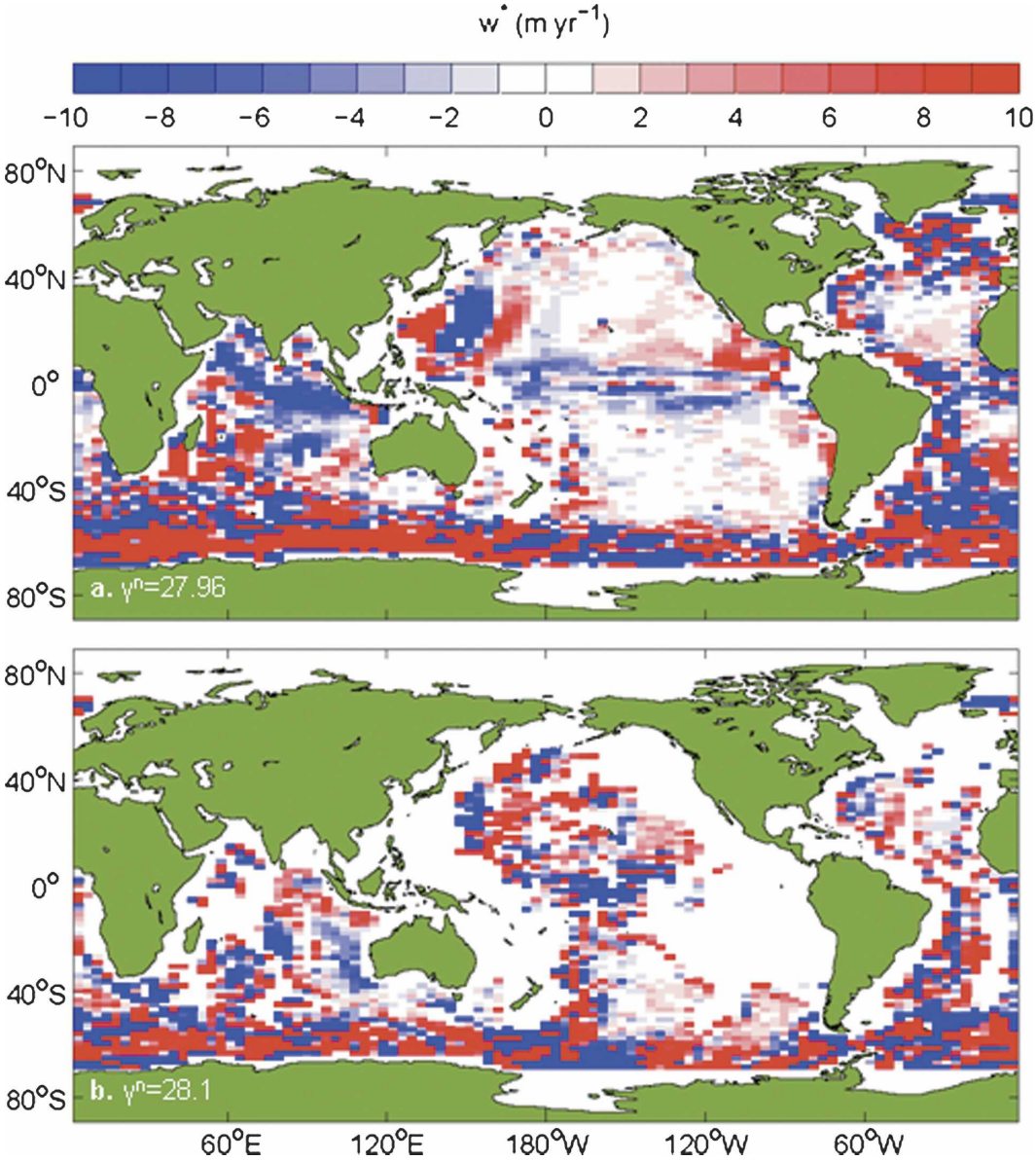

FIG. 4. Map of diapycnal advection w^* for the (a) $\gamma^n = 27.96$ and (b) 28.1 kg m^{-3} surfaces of the OGCM numerical simulations of Simmons et al. (2004). The model employs a spatially variable diffusivity that averages to (1–3) $\times$ 10^{-4} m^2 s^{-1} for the deep- and bottom-water masses (cf. Table 2, case B). Vertical velocity amplitudes greater than 10 m yr^{-1} are saturated on the color axis as a means of accentuating the patterns of upwelling and downwelling.

work done on the oceans by the astronomical forcing of the earth–moon–sun system is roughly 3.5 TW (Munk and Wunsch 1998). Roughly 2.5 TW of tidal energy is dissipated in shallow seas, leaving roughly 1 TW for deep-ocean conversion to internal tides (Egbert and Ray 2000; Jayne and St. Laurent 2001). Net primary production accounts for roughly 60 TW of carbohydrate energy. Most of this energy is used in chemical form by animals in the biosphere, but Dewar et al. (2006) suggest that $O(1)$ TW is likely converted to biomechanical work done by organisms swimming in the aphotic ocean. This estimate has considerable uncertainty.

Thus, we conclude that 3 TW is both a reasonable estimate for the power required to support observed mixing rates in the ocean interior, and is also consistent with existing estimates for available energy sources. However, open questions remain regarding all aspects

of energy input, cascade processes, and dissipation, including their role in the ocean's thermohaline circulation.

Acknowledgments. We thank B. Dewar, R. Ferrari, S. Jayne, E. Kunze, T. McDougall, and two anonymous reviewers for helpful comments on this work. The authors are supported by grants from the U.S. Office of Naval Research and the National Science Foundation.

REFERENCES

Alford, M. H., 2001: Internal swell generation: The spatial distribution of energy flux from the wind to mixed-layer near-inertial motions. *J. Phys. Oceanogr.,* **31,** 2359–2368.

——, 2003: Improved global maps and 54-year history of wind work on ocean inertial motions. *Geophys. Res. Lett.,* **30,** 1424, doi:10.1029/2002GL016614.

Arneborg, L., 2002: Mixing efficiencies in patch turbulence. *J. Phys. Oceanogr.,* **32,** 1496–1506.

Bevington, P. R., and D. K. Robinson, 1992: *Data Reduction and Error Analysis for the Physical Sciences.* McGraw-Hill, 328 pp.

Bryan, F., 1987: Parameter sensitivity of primitive equation ocean general circulation models. *J. Phys. Oceanogr.,* **17,** 970–985.

Bryden, H. L., and A. J. G. Nurser, 2003: Effects of strait mixing on ocean stratification. *J. Phys. Oceanogr.,* **33,** 1870–1872.

Canuto, V. M., A. Howard, Y. Cheng, and M. S. Dubovikov, 2002: Ocean turbulence. Part II: Vertical diffusivities of momentum, heat, salt, mass, and passive scalars. *J. Phys. Oceanogr.,* **32,** 240–264.

Davis, R. E., 1994: The Osborn–Cox model. *J. Phys. Oceanogr.,* **24,** 2560–2576.

——, 1996: Sampling turbulent dissipation. *J. Phys. Oceanogr.,* **26,** 341–358.

Dewar, W. K., R. J. Bingham, R. L. Iverson, D. P. Nowacek, L. C. St. Laurent, and P. H. Wiebe, 2006: Marine bioturbation. *J. Mar. Res.,* **64,** 553–573.

Egbert, G. D., and R. D. Ray, 2000: Significant dissipation of tidal energy in the deep ocean inferred from satellite altimeter data. *Nature,* **405,** 775–778.

Ferron, B., H. Mercier, K. Speer, A. Gargett, and K. Polzin, 1998: Mixing in the Romanche Fracture Zone. *J. Phys. Oceanogr.,* **28,** 1929–1945.

Fofonoff, N. P., 1985: Physical properties of seawater: A new salinity scale and equation of state for seawater. *J. Geophys. Res.,* **90,** 3332–3342.

Ganachaud, A., and C. Wunsch, 2000: Improved estimates of global circulation, heat transport and mixing from hydrographic data. *Nature,* **408,** 453–457.

Gnanadesikan, A., R. D. Slater, P. S. Swathi, and G. K. Vallis, 2005: The energetics of ocean heat transport. *J. Climate,* **18,** 2604–2616.

Gregg, M. C., 1987: Diapycnal mixing in the thermocline: A review. *J. Geophys. Res.,* **92,** 5249–5286.

——, 1989: Scaling turbulent dissipation in the thermocline. *J. Geophys. Res.,* **94,** 9686–9698.

Griffies, S., R. Pacanowski, and R. Hallberg, 2000: Spurious diapycnal mixing associated with advection in a z-coordinate ocean model. *Mon. Wea. Rev.,* **128,** 538–564.

Hasumi, H., and N. Suginohara, 1999: Effects of locally enhanced vertical diffusivity over rough bathymetry on the world ocean circulation. *J. Geophys. Res.,* **104,** 23 367–23 374.

Heywood, K. J., A. C. Naveira Garabato, and D. P. Stevens, 2002: High mixing rates in the abyssal Southern Ocean. *Nature,* **415,** 1011–1014.

Hibiya, T., M. Nagasawa, and Y. Niwa, 2002: Nonlinear energy transfer within the oceanic internal wave spectrum at mid and high latitudes. *J. Geophys. Res.,* **107,** 3207, doi:10.1029/2001JC001210.

Hogg, N. G., P. Biscaye, E. Gardner, and W. J. Schmitz, 1982: On the transport of Antarctic Bottom Water in the Vema Channel. *J. Mar. Res.,* **40** (Suppl.), 231–263.

Hughes, C. O., and R. W. Griffiths, 2006: A simple convective model of the global overturning circulation, including effects of entrainment into sinking regions. *Ocean Modell.,* **12,** 46–79.

Huq, P., and R. E. Britter, 1995: Turbulence evolution and mixing in a two layer stably stratified fluid. *J. Fluid Mech.,* **285,** 41–67.

Jackett, D. R., and T. J. McDougall, 1997: A neutral density variable for the world's oceans. *J. Phys. Oceanogr.,* **27,** 237–263.

Jayne, S. R., and L. C. St. Laurent, 2001: Parameterizing tidal dissipation over rough topography. *Geophys. Res. Lett.,* **28,** 811–814.

Kerr, R. A., 2000: Missing mixing found in the deep sea. *Science,* **288,** 1947–1949.

Klymak, J. M., and Coauthors, 2006: An estimate of tidal energy lost to turbulence at the Hawaiian Ridge. *J. Phys. Oceanogr.,* **36,** 1148–1164.

Kolmogorov, A. N., 1941: The local structure of turbulence in incompressible viscous fluid for very large Reynolds numbers. *Dokl. Akad. Nauk. SSSR,* **32,** 16–18.

Kunze, E., and J. M. Toole, 1997: Tidally driven vorticity, diurnal shear, and turbulence atop Fieberling Seamount. *J. Phys. Oceanogr.,* **27,** 2663–2693.

——, E. Firing, J. M. Hummon, T. K. Chereskin, and A. M. Thurnherr, 2006: Global abyssal mixing inferred from lowered ADCP shear and CTD strain profiles. *J. Phys. Oceanogr.,* in press.

Ledwell, J. R., A. J. Watson, and C. S. Law, 1993: Evidence for slow mixing across the pycnocline from an open-ocean tracer-release experiment. *Nature,* **364,** 701–703.

Levitus, S., and T. P. Boyer, 1994: *Temperature.* Vol. 4, *World Ocean Atlas 1994,* NOAA Atlas NESDIS 4, 117 pp.

——, R. Burgett, and T. P. Boyer, 1994: *Salinity.* Vol. 3, *World Ocean Atlas 1994,* NOAA Atlas NESDIS 3, 99 pp.

Lueck, R., and R. Reid, 1984: On the production and dissipation of mechanical energy in the ocean. *J. Geophys. Res.,* **89,** 3439–3445.

Lueck, R. G., and T. D. Mudge, 1997: Topographically induced mixing around a shallow seamount. *Science,* **276,** 1831–1833.

——, F. Wolk, and H. Yamazaki, 2002: Oceanic velocity microstructure measurements in the 20th Century. *J. Oceanogr.,* **58,** 153–174.

Lumpkin, R., and K. Speer, 2003: Large-scale vertical and horizontal circulation in the North Atlantic Ocean. *J. Phys. Oceanogr.,* **33,** 1902–1920.

MacDonald, A., and C. Wunsch, 1996: The global ocean circulation and heat flux. *Nature,* **382,** 436–439.

Marshall, J., and T. Radko, 2003: Residual-mean solutions for the

Antarctic Circumpolar Current and its associated overturning circulation. *J. Phys. Oceanogr.,* **33,** 2341–2354.

Mauritzen, C., K. L. Polzin, M. S. McCartney, R. C. Millard, and D. E. West-Mack, 2002: Evidence in hydrography and density fine structure for enhanced vertical mixing over the mid-Atlantic Ridge in the western Atlantic. *J. Geophys. Res.,* **107,** 3147, doi:10.1029/2001JC001114.

Millard, R. C., W. B. Owens, and N. P. Fofonoff, 1990: On the calculation of Brunt-Vaisala frequency. *Deep-Sea Res.,* **37,** 167–181.

Morris, M. Y., M. M. Hall, L. C. St. Laurent, and N. G. Hogg, 2001: Abyssal mixing in the Brazil Basin. *J. Phys. Oceanogr.,* **31,** 3331–3348.

Moum, J. N., 1996: Efficiency of mixing in the main thermocline. *J. Geophys. Res.,* **101,** 12 057–12 069.

——, and T. R. Osborn, 1986: Mixing in the main thermocline. *J. Phys. Oceanogr.,* **16,** 1250–1259.

Munk, W. H., 1966: Abyssal recipes. *Deep-Sea Res.,* **13,** 207–230.

——, and C. Wunsch, 1998: Abyssal recipes II: Energetics of tidal and wind mixing. *Deep-Sea Res.,* **45,** 1977–2010.

Naveira Garabato, A. C., K. L. Polzin, B. A. King, K. J. Heywood, and M. Visbeck, 2004: Widespread intense turbulent mixing in the Southern Ocean. *Science,* **303,** 210–213.

Oakey, N. S., 1985: Statistics of mixing parameters in the upper ocean during JASIN Phase 2. *J. Phys. Oceanogr.,* **15,** 1662–1675.

Olbers, D., and J. Wenzel, 1989: Determining diffusivities from hydrographic data using inverse methods with application to the Circumpolar Current. *Ocean Circulation Models: Combining Data with Dynamics*, D. Anderson and J. Willebrand, Eds., Kluwer, 95–140.

Osborn, T. R., 1980: Estimates of the local rate of vertical diffusion from dissipation measurements. *J. Phys. Oceanogr.,* **10,** 83–89.

——, and C. S. Cox, 1972: Oceanic fine structure. *Geophys. Fluid Dyn.,* **3,** 321–345.

Peltier, W. R., and C. P. Caulfield, 2003: Mixing efficiency in stratified shear flows. *Annu. Rev. Fluid Mech.,* **35,** 135–167.

Peters, H., M. C. Gregg, and J. M. Toole, 1989: Meridional variability of turbulence through the equatorial undercurrent. *J. Geophys. Res.,* **94,** 18 003–18 009.

——, ——, and T. B. Sanford, 1994: The diurnal cycle of the upper equatorial ocean: Turbulence, fine-scale shear, and mean shear. *J. Geophys. Res.,* **99,** 7707–7723.

Polzin, K., E. Kunze, J. Hummon, and E. Firing, 2002: The fine-scale response of lowered ADCP velocity profiles. *J. Atmos. Oceanic Technol.,* **19,** 205–224.

Polzin, K. L., and E. Firing, 1997: Estimates of diapycnal mixing using LADCP and CTD data from I8S. *WOCE Notes,* **29,** 39–42.

——, J. M. Toole, and R. W. Schmitt, 1995: Finescale parameterizations of turbulent dissipation. *J. Phys. Oceanogr.,* **25,** 306–328.

Robinson, A. R., and H. Stommel, 1959: The oceanic thermocline and the associated thermohaline circulation. *Tellus,* **11,** 295–308.

Rohr, J. J., and C. W. Van Atta, 1987: Mixing efficiency in stably stratified growing turbulence. *J. Geophys. Res.,* **92,** 5481–5488.

Samelson, R. M., and G. K. Vallis, 1997: Large-scale circulation with small diapycnal diffusion: The two-thermocline limit. *J. Mar. Res.,* **55,** 223–275.

Schmitt, R. W., J. R. Ledwell, E. T. Montgomery, K. L. Polzin, and J. M. Toole, 2005: Enhanced diapycnal mixing by salt fingers in the thermocline of the tropical Atlantic. *Science,* **308,** 685–688.

Simmons, H. L., S. R. Jayne, L. C. St. Laurent, and A. J. Weaver, 2004: Tidally driven mixing in a numerical model of the general circulation. *Ocean Modell.,* **6,** 245–263.

Smith, D. K., and D. Sandwell, 1997: Global sea floor topography from satellite altimetry and ship depth soundings. *Science,* **277,** 1956–1962.

Stigebrandt, A., and J. Aure, 1989: On vertical mixing in the basin waters of Fjords. *J. Phys. Oceanogr.,* **19,** 917–926.

St. Laurent, L. C., and R. W. Schmitt, 1999: The contribution of salt fingers to vertical mixing in the North Atlantic Tracer Release Experiment. *J. Phys. Oceanogr.,* **29,** 1404–1424.

——, J. M. Toole, and R. W. Schmitt, 2001: Buoyancy forcing by turbulence above rough topography in the abyssal Brazil Basin. *J. Phys. Oceanogr.,* **31,** 3476–3495.

Stommel, H., 1957: The abyssal circulation of the ocean. *Nature,* **180,** 733–734.

——, and F. Schott, 1977: The beta spiral and the determination of the absolute velocity field from hydrographic station data. *Deep-Sea Res.,* **24,** 325–329.

Thompson, R. O. R. Y., 1980: Efficiency of conversion of kinetic energy to potential energy by a breaking internal gravity wave. *J. Geophys. Res.,* **85,** 6631–6635.

Thurnherr, A. M., L. C. St. Laurent, K. G. Speer, J. M. Toole, and J. R. Ledwell, 2005: Mixing associated with sills in canyons on the mid-ocean ridge flank. *J. Phys. Oceanogr.,* **35,** 1370–1381.

Toggweiler, J. R., and B. Samuels, 1998: On the ocean's large scale circulation near the limit of no vertical mixing. *J. Phys. Oceanogr.,* **28,** 1832–1852.

Toole, J. M., K. L. Polzin, and R. W. Schmitt, 1994: Estimates of diapycnal mixing in the abyssal ocean. *Science,* **264,** 1120–1123.

Wang, W., and R. Huang, 2004a: Wind energy input to the Ekman layer. *J. Phys. Oceanogr.,* **34,** 1267–1275.

——, and ——, 2004b: Wind energy input to the surface waves. *J. Phys. Oceanogr.,* **34,** 1276–1280.

Webb, D. J., and N. Suginohara, 2001a: Vertical mixing in the ocean. *Nature,* **49,** 37–38.

——, and ——, 2001b: The interior circulation of the ocean. *Ocean Circulation and Climate,* G. Siedler, J. Church, and J. Gould, Eds., Academic Press, 205–214.

Wunsch, C., 1978: The North Atlantic general circulation west of 50° determined by inverse methods. *Rev. Geophys. Space Phys.,* **16,** 583–620.

——, 1996: *The Ocean Circulation Inverse Problem*. Cambridge University Press, 442 pp.

——, 1998: The work done by the wind on the oceanic general circulation. *J. Phys. Oceanogr.,* **28,** 2332–2342.

Wyrtki, K., 1961: The thermohaline circulation in relation to the general circulation in the oceans. *Deep-Sea Res.,* **8,** 39–64.